Evolution has strong medicine for antibiotics use *p. 758*

The personal costs of healing societies *pp. 766 & 787*

A call to counter hype in stem cell research *p. 776*

Science

$15
13 MAY 2016
sciencemag.org

AAAS

A MIGRANT'S PLIGHT

Arctic warming hurts red knots on their tropical winter range *pp. 775 & 819*

CLIMATE CHANGE

Body shrinkage due to Arctic warming reduces red knot fitness in tropical wintering range

Jan A. van Gils,[1*] Simeon Lisovski,[2] Tamar Lok,[3,4] Włodzimierz Meissner,[5] Agnieszka Ożarowska,[5] Jimmy de Fouw,[1] Eldar Rakhimberdiev,[1,6] Mikhail Y. Soloviev,[6] Theunis Piersma,[1,3] Marcel Klaassen[2]

Reductions in body size are increasingly being identified as a response to climate warming. Here we present evidence for a case of such body shrinkage, potentially due to malnutrition in early life. We show that an avian long-distance migrant (red knot, *Calidris canutus canutus*), which is experiencing globally unrivaled warming rates at its high-Arctic breeding grounds, produces smaller offspring with shorter bills during summers with early snowmelt. This has consequences half a world away at their tropical wintering grounds, where shorter-billed individuals have reduced survival rates. This is associated with these molluscivores eating fewer deeply buried bivalve prey and more shallowly buried seagrass rhizomes. We suggest that seasonal migrants can experience reduced fitness at one end of their range as a result of a changing climate at the other end.

Phenological changes and geographical range shifts are well-known responses to climate change (*1*). A third broadly observed response to global warming appears to be shrinkage of bodies (*2*–*5*). It has been hypothesized that body shrinkage is a genetic microevolutionary response to warming, due to smaller individuals being better able to dissipate body heat because of the larger surface/volume ratio of their bodies [e.g., Bergmann's rule (*2*)]. Alternatively, it has been put forward that climate change may disrupt trophic interactions, potentially leading to malnutrition during an organism's juvenile life stage (*6*, *7*). Because poor growth may not be compensated for later in life (*8*), this would lead to smaller bodies (i.e., shrinkage as a phenotypically plastic response).

Under climate change, some regions are warming faster than others. Especially in the Arctic, warming has been observed at unprecedented rates (*9*, *10*). Hence, body-size reductions would be expected to be most pronounced in the world's most northerly region (*6*). Many Arctic-breeding avian species, however, are long-distance migrants that spend the northern winter at lower latitudes (*11*), where the impacts of climate change are less obvious.

Based on analysis of satellite data, we show here that over the past 33 years, snowmelt has occurred progressively earlier in the high-Arctic breeding grounds of the red knot (*Calidris canutus canutus*) at Taimyr Peninsula (76° to 78°N; Fig. 1), changing at a rate of about half a day per year [coefficient of determination (R^2) = 0.32, $F_{1,31}$ = 14.77, P < 0.001; Fig. 2A, table S1, and figs. S1 to S3]. Over these three decades, 1990 juvenile red knots were caught and their body sizes measured in Gdańsk Bay, Poland, during their first southward migration to their West African nonbreeding grounds (Fig. 1). These measurements show that juvenile birds were smaller after Arctic summers with early snowmelts, particularly with respect to body mass [corrected Akaike information criterion (AIC_c) = 14775.24, P < 0.0005; Fig. 2B and table S2], bill length (AIC_c = 7610.48, P < 0.005; Fig. 2C and table S3), and overall body size [first principal component (PC1) on bill, tarsus, and wing; AIC_c = 5925.22, P < 0.05; table S4]. The models that best explained the variation in bill length and overall body size additionally included the Normalized Difference Vegetation Index [NDVI, a proxy for total primary biomass production (*12*)] of the breeding ground; longer-billed, bigger birds were captured after summers with high NDVI values (Fig. 2C). These size variations were still apparent when juveniles arrived at their main wintering ground on the Banc d'Arguin, Mauritania (annual average juvenile bill lengths in Poland and Mauritania correlated strongly: Pearson's r = 0.73), where red knots showed no signs of compensatory growth (measurements of body size dimensions, including bill length, were highly consistent within individuals; fig. S4B).

In this tropical nonbreeding area, red knots use their tapered bills to detect and retrieve mollusk prey buried in intertidal sediments (*13*). Stable isotope analysis of 2340 birds caught at Banc d'Arguin between 2002 and 2013 shows that longer-billed birds relied mostly on the abundant bivalve prey species *Loripes lucinalis* (hereafter, *Loripes*), whereas shorter-billed individuals did not (R^2 = 0.18, $F_{3,2336}$ =170.70, P < 0.00001; Fig. 3A). This may be due to most *Loripes* being buried out of reach for shorter-billed knots: An individual with a 40-mm bill has access to about two-thirds of all *Loripes*, whereas a bird with a 30-mm bill is able to access only one-third (Fig. 3B). Shorter-billed red knots consumed relatively more of the shallowly buried bivalve *Dosinia isocardia* (hereafter, *Dosinia*) and rhizomes of the seagrass *Zostera noltii* (hereafter, *Zostera*; Fig. 3B and fig. S5). Juvenile red knots consumed fewer *Loripes* compared with older birds (P < 0.00001 for the age-bill interaction; Fig. 3A). This is probably due to the fact that *Loripes* is mildly toxic; the sulphide metabolism of endosymbiotic bacteria living inside its gill causes diarrhea (*14*). In spite of its toxic effects, red knots depend on *Loripes*, especially in years with few alternatives (*15*). Juveniles may need physiological adjustments before they can digest this special type of prey efficiently (*16*). Only birds with longer bills can make this switch to eating the deeply buried *Loripes*; the shorter-billed birds are restricted to a "juvenile diet" of relatively rare *Dosinia (15)* and poor-quality rhizomes (*17*). Hence, for the shorter-billed birds, the inability to access the high-quality and abundant *Loripes* after the first winter may come at a cost.

Individual color-ringing of 2381 red knots during annual expeditions to Banc d'Arguin from 2002 to 2013, and subsequent resightings of these individuals (*12*), indicate that birds with shorter bills had lower apparent survival rates, primarily in the case of juveniles between their first and second winters [Fig. 4A, fig. S6, and tables S5 to S8; we use the term "apparent survival" because mortality is confounded with permanent emigration (*18*)]. The much weaker bill-length effect in adults may be attributable to the advantages of a short bill when feeding on arthropods on the tundra (*19*); juveniles do not benefit from these advantages because they stay at the Mauritanian nonbreeding grounds year-round (*20*). Because early-snowmelt years produced shorter-billed juveniles (Fig. 2C), and because shorter-billed juveniles experienced hampered survival in the tropics (Fig. 4A), overwintering juveniles thus had poor survival rates after Arctic summers with early snowmelt [proportion of variation explained by date of snowmelt (R^2_{dev}) = 0.32 (*12*); Fig. 4B]. However, with snowmelt occurring progressively earlier over the years (Pearson's r = –0.58 for 2002–2012), the temporal variation in juvenile survival was similarly well explained by a linear time trend (model 13 versus 14, ΔAIC_c=1.01; table S7). Strictly speaking, we therefore cannot distinguish an effect of snowmelt date on survival from any other potential covariate changing over time. We see this problem as inherent to any descriptive study of climate change effects.

[1]Department of Coastal Systems, NIOZ Royal Netherlands Institute for Sea Research, and Utrecht University, Post Office Box 59, 1790 AB Den Burg (Texel), Netherlands. [2]Centre for Integrative Ecology, School of Life and Environmental Sciences, Deakin University, Waurn Ponds Campus, Victoria 3217, Australia. [3]Conservation Ecology Group, Groningen Institute for Evolutionary Life Sciences (GELIFES), University of Groningen, Post Office Box 11103, 9700 CC Groningen, Netherlands. [4]Centre d'Ecologie Fonctionnelle et Evolutive, Unité Mixte de Recherche 5175, Campus Centre National de la Recherche Scientifique, 1919 Route de Mende, 34293 Montpellier Cedex 5, France. [5]Avian Ecophysiology Unit, Department of Vertebrate Ecology and Zoology, University of Gdańsk, Wita Stwosza 59, 80-308 Gdańsk, Poland. [6]Department of Vertebrate Zoology, Lomonosov Moscow State University, Moscow, 119991, Russia.
***Corresponding author. Email: jan.van.gils@nioz.nl**

In the face of climate change–induced body shrinkage and the strong selection pressure against shorter-billed juveniles at the nonbreeding grounds, one would expect the adult population to maintain a relatively constant bill length or at least to show less shrinkage of the bill compared with other structural body-size components. This was the case (fig. S7): Although overall body size (PC1 on bill, tarsus, and wing) in adults decreased at a rate of 0.020 SDs per year (R^2 = 0.26, $F_{2,1727}$ = 299.20, P < 0.001), their bill length decreased at a rate of only 0.010 SDs per year (R^2 = 0.21, $F_{2,1727}$ = 223.57, P = 0.097), suggesting a climate change–induced directional selection on body shape.

The body shrinkage observed in juvenile red knots may be a phenotypically plastic response to an altered environment. Neonatal red knots feed on arthropods (*21*) that emerge from a defrosting tundra soil (*22*). With the rapid advancement in the seasonal appearance of high-Arctic arthropods (*23*), red knot chicks may face a trophic mismatch by hatching too late relative to the peak food abundance (*23*)—in spite of evidence for earlier nesting in high-Arctic shorebirds (*24*), and in spite of the observation that red knot spring migration through France is advancing [although at only 0.25 days/year, which is half the rate at which the timing of snowmelt is advancing) (*25*)]. In addition to advancing the timing of the arthropod peak, earlier snowmelts are also known to depress the peak's amplitude. This is because earlier snowmelts produce smaller-bodied insects (*26*) and cause greater soil temperature fluctuations, thereby enhancing mortality among larvae (*27*). Our finding that bills and bodies are smaller in years with low breeding-ground NDVI values (Fig. 2C) hints at the importance of the food peak's amplitude, because low NDVI values are considered to reflect low insect abundances (*28*).

The negative effects of climate change on the growth of red knots may thus be due to a trophic mismatch. The fitness-related consequences of this growth inhibition are that smaller, shorter-billed individuals have, on average, reduced apparent survival rates at their tropical wintering grounds. This mechanism may be one of the drivers of the steep and ongoing population decline of the *C. c. canutus* red knots (*15*, *29*). The discovery of rapid body shrinkage and its downstream effects on population size may extend to other Arctic migrants.

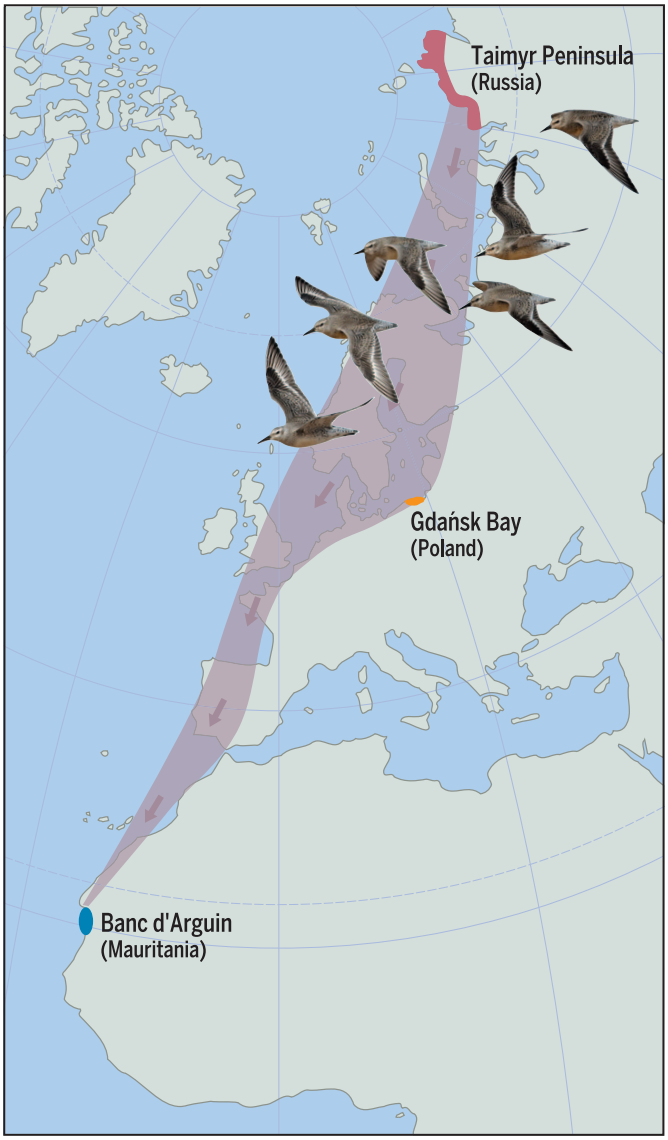

Fig. 1. Red knots breed during summer in the high Arctic at Taimyr Peninsula and spend the long nonbreeding season at Banc d'Arguin, Mauritania, West Africa. On their first southward migration to West Africa, many juvenile red knots make a stopover on the Baltic coast of Poland.

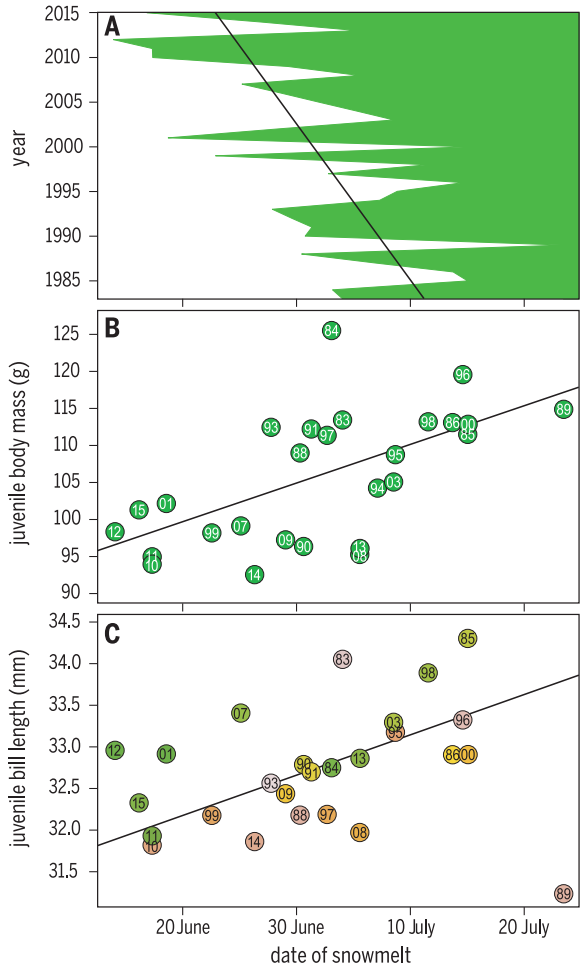

Fig. 2. Changes in Arctic climate and red knot body size over the past three decades. (**A**) Snow at the red knots' breeding ground at Taimyr Peninsula has been melting progressively earlier at an average rate of 0.5 days/year. (**B**) Juvenile red knots, captured during brief stopovers in Poland on their first southward migration from the Arctic, had lower body masses after breeding seasons in which snow had disappeared early (each circle denotes the annual mean, with number inside the circle giving the year). (**C**) They also had shorter bills after breeding seasons in which the Arctic snow melted earlier [circles denote annual means as in (B)], especially in years when breeding-ground NDVI [as a proxy for total primary biomass production (*12*)] was low [NDVI is indicated by the color range of the circles (green, high; pink, low)].

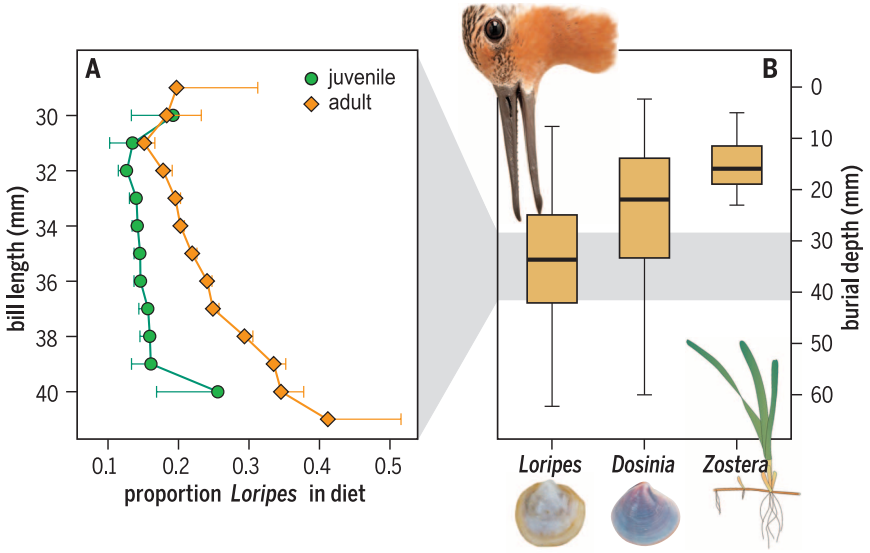

Fig. 3. Prey choice and prey availability at the Mauritanian wintering grounds. (**A**) Analysis of stable isotopes of blood samples shows that juvenile red knots (n = 676 birds) largely ignored the most abundant but mildly toxic prey, *Loripes*. However, with an increase in age, adult red knots (n = 1664) added substantial amounts of *Loripes* to their diet, but only if they had long bills. Plotted are means ± SE. (**B**) This bill length–dependent diet shift may be explained by the depth distribution of *Loripes*. The majority of these bivalves live between 30 and 40 mm below the seafloor, which is precisely the range of the bill lengths. The other two food sources, *Dosinia* bivalves and *Zostera* rhizomes, are found at shallower depths and are accessible to all red knots. Bars indicate medians, boxes indicate 25th to 75th percentiles, and whiskers indicate ranges.

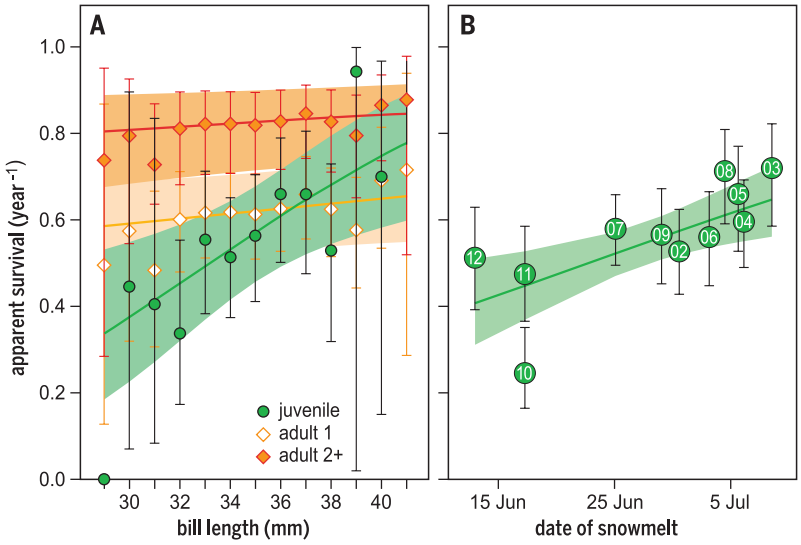

Fig. 4. Annual survival rates of individually marked red knots. (**A**) Annual apparent survival rates [± 95% confidence intervals (CIs)] increase significantly as a function of bill length in juveniles (the slope β of the relationship of logit-transformed values = 0.30; 95% CI, 0.08 to 0.51; n = 690 birds), whereas this relation is not significant for adults [β = 0.05; 95% CI, −0.02 to 0.11; n = 1691 birds; distinguishing between survival in the first year after capture (adult 1) and later (adult 2+)]. Symbols show apparent survival rates of juveniles born in 2009 (a year with average survival; model 11, table S7); lines show these data as a linear function of bill length [model 1 (the best-supported model), table S7]. Shaded areas are 95% CIs of the linear functions. Bill-length effect is assumed to be the same in all years. (**B**) Annual apparent survival rates (± 95% CIs) of juveniles increase with the date of snowmelt in their year of birth (the year is indicated inside the circle). Symbols show juvenile apparent survival rates estimated per year (model 8, table S7); lines show these data as a linear function of the date of snowmelt (model 14, table S7). Time dependence in both the apparent survival and resighting makes the survival estimate for the final year (i.e., for juveniles born in 2013) unreliable; hence, this estimate was excluded.

REFERENCES AND NOTES

1. C. Parmesan, G. Yohe, *Nature* **421**, 37–42 (2003).
2. C. Teplitsky, V. Millien, *Evol. Appl.* **7**, 156–168 (2014).
3. A. R. Baudron, C. L. Needle, A. D. Rijnsdorp, C. T. Marshall, *Glob. Change Biol.* **20**, 1023–1031 (2014).
4. J. A. Sheridan, D. Bickford, *Nat. Clim. Change* **1**, 401–406 (2011).
5. J. L. Gardner, A. Peters, M. R. Kearney, L. Joseph, R. Heinsohn, *Trends Ecol. Evol.* **26**, 285–291 (2011).
6. K. D. Rode, S. C. Amstrup, E. V. Regehr, *Ecol. Appl.* **20**, 768–782 (2010).
7. C. Teplitsky, J. A. Mills, J. S. Alho, J. W. Yarrall, J. Merilä, *Proc. Natl. Acad. Sci. U.S.A.* **105**, 13492–13496 (2008).
8. N. B. Metcalfe, P. Monaghan, *Trends Ecol. Evol.* **16**, 254–260 (2001).
9. M. P. Tingley, P. Huybers, *Nature* **496**, 201–205 (2013).
10. J. A. Screen, I. Simmonds, *Nature* **464**, 1334–1337 (2010).
11. T. Piersma, *Oikos* **80**, 623–631 (1997).
12. Materials and methods are available as supplementary materials on *Science* Online.
13. T. Piersma, R. van Aelst, K. Kurk, H. Berkhoudt, L. R. M. Maas, *Proc. Biol. Sci.* **265**, 1377–1383 (1998).
14. T. Oudman *et al.*, *Am. Nat.* **183**, 650–659 (2014).
15. J. A. van Gils *et al.*, *Proc. Biol. Sci.* **280**, 20130861 (2013).
16. R. W. Stein, A. R. Place, T. Lacourse, C. G. Guglielmo, T. D. Williams, *Physiol. Biochem. Zool.* **78**, 434–446 (2005).
17. J. L. Pérez-Lloréns, M. Muchtar, F. X. Niell, P. H. Nienhuis, *Bot. Mar.* **34**, 319–322 (1991).
18. J. D. Lebreton, K. P. Burnham, J. Clobert, D. R. Anderson, *Ecol. Monogr.* **62**, 67–118 (1992).
19. P. E. Jönsson, T. Alerstam, *Biol. J. Linn. Soc. Lond.* **41**, 301–314 (1990).
20. A. J. van Dijk, F. E. de Roder, E. C. L. Marteijn, H. Spiekman, *Ardea* **78**, 145–156 (1990).
21. H. Schekkerman, I. Tulp, T. Piersma, G. H. Visser, *Oecologia* **134**, 332–342 (2003).
22. H. V. Danks, *Eur. J. Entomol.* **96**, 83–102 (1999).
23. T. T. Høye, E. Post, H. Meltofte, N. M. Schmidt, M. C. Forchhammer, *Curr. Biol.* **17**, R449–R451 (2007).
24. J. R. Liebezeit, K. E. B. Gurney, M. Budde, S. Zack, D. Ward, *Polar Biol.* **37**, 1309–1320 (2014).
25. J. Leyrer *et al.*, *Wader Study Group Bull.* **116**, 145–151 (2009).
26. J. J. Bowden *et al.*, *Biol. Lett.* **11**, 20150574 (2015).
27. J. S. Bale, S. A. L. Hayward, *J. Exp. Biol.* **213**, 980–994 (2010).
28. M. P. Grilli, D. E. Gorla, *Bull. Entomol. Res.* **87**, 45–53 (1997).
29. M. van Roomen, S. Nagy, R. Foppen, T. Dodman, G. Citegetse, A. Ndiaye, *Status of Coastal Waterbird Populations in the East Atlantic Flyway* (Programme Rich Wadden Sea, Sovon, Wetlands International, Birdlife International, Common Wadden Sea Secretariat, 2015).

ACKNOWLEDGMENTS

This paper was conceptualized during J.A.v.G.'s sabbatical at the Centre for Integrative Ecology at Deakin University and benefited greatly from discussions with Y. Aharon-Rotman and B. J. Hoye at Deakin University; discussions with A. I. Bijleveld, S. Duijns, E. M. A. Kok, and T. Oudman at NIOZ; and comments by three anonymous referees. We thank W. Bouma and F. Sanders for wordsmithing and D. Visser for graphical support. Field support was provided by Waterbird Research Group KULING in the Polish Baltic and the Banc d'Arguin teams led by B. Spaans, J. Leyrer, M. Brugge, A. Dekinga, and J. ten Horn; we were hosted at Iwik by Parc National du Banc d'Arguin (PNBA) staff (notably M. Camara). We thank the directors of the PNBA for access to the study area. Stable isotope analyses were conducted by T. Leerink, J. Ossebaar, and K. Donkers. Financial support was provided by a NWO (Netherlands Organisation for Scientific Research) Vidi grant (864.09.002) to J.A.v.G., NWO-Rubicon funding to T.L., a suite of grants to T.P. [Waddenfonds project Metawad (WF209925), BirdLife Netherlands, World Wildlife Fund–Netherlands, the Prins Bernhard Cultuurfondsprijs voor Natuurbehoud, NWO-WOTRO (Science for Global Development) Integrated Programme (W.01.65.221.00), and MAVA (Switzerland)], and a grant from the Australian Research Council (DP130101935) to M.K. Data and R codes are available at Dryad at http://dx.doi.org/10.5061/dryad.n1m8d.

SUPPLEMENTARY MATERIALS

www.sciencemag.org/content/352/6287/819/suppl/DC1
Materials and Methods
Figs. S1 to S7
Tables S1 to S8
References (*30–54*)

14 October 2015; accepted 5 April 2016
10.1126/science.aad6351

www.sciencemag.org/content/352/6287/819/suppl/DC1

Supplementary Materials for

Body shrinkage due to Arctic warming reduces red knot fitness in tropical wintering range

Jan A. van Gils,* Simeon Lisovski, Tamar Lok, Włodzimierz Meissner, Agnieszka Ożarowska, Jimmy de Fouw, Eldar Rakhimberdiev, Mikhail Y. Soloviev, Theunis Piersma, Marcel Klaassen

*Corresponding author. Email: jan.van.gils@nioz.nl

Published 13 May 2016, *Science* **352**, 819 (2016)
DOI: 10.1126/science.aad6351

This PDF file includes:

Supplementary Materials: Methods

High-Arctic climatic data (Taimyr Peninsula)

Temperature data

Daily mean temperatures were obtained for 1983-2015 across the entire breeding range of the *Calidris c. canutus* subspecies (northern Taimyr Peninsula as defined by Lappo *et al*. (*30*)). Following the methodology outlined elsewhere (*31*), daily temperature data (May-August) were downloaded from the NOAA National Climatic Data Centre (*32*), which were then plotted as temperature surface maps (*33*), using 'gravity' as the interpolation algorithm, while taking a search radius of 500 km and a maximum of ten weather stations. Subsequently, daily surface maps were overlaid on the knot's breeding range, and surface values were averaged across this range, yielding a mean temperature for each day. Next, for each year separately, a quadratic model was fitted to these daily mean temperatures (using the *lm* function in R) (*34*), and the date at which the increasing part of this fit reached 0 °C was defined as D_{T0}. An example of this procedure is given in Fig. S1, with all estimates for D_{T0} listed in Table S1.

Snow cover data

Based on the remotely sensed NOAA CDR climate dataset, weekly snow and ice cover data for the period 1983-2015 on a scale of 24 × 24 km were downloaded (*32, 35*). Next, grid cells falling in the subspecies' entire breeding range were extracted. Next, large erratic changes in snow cover during summer were removed as these reflect rather unpredictable incidences and do not reflect the main phenology of the seasonal snowfall-thaw cycle. Then, data were modelled using a maximum likelihood fit (*mle2* function from R package *bbmle*) of the asymmetric Gaussian model function (*36*) with a binomial error distribution. Using these year-specific fits, date of snowmelt D_{SM} was then determined as the date on which the fitted curve predicted 1/3 of the whole area to be snow free, whereas date of snowfall D_{SF} was determined as the predicted date when 1/3 of the whole area was covered by snow. An example of the latter procedure is given in Fig. S2, with all phenology indices listed in Table S1.

Normalized Difference Vegetation Index (NDVI) data

From the NOAA STAR AVHRR Vegetation Health dataset, weekly raw NDVI data on a scale of 16 × 16 km grid cells were downloaded for the period 1983-2015 (*37*). Next, cells located in the subspecies' entire breeding range were selected for further analysis. Then, for each year separately, a smoother was fitted through the data (using the *loess* function in R, span set to 0.3), where after values due to the albedo effect of snow cover were removed: in case the smoother decreased in spring before reaching the summer maximum and increased in autumn then the values before the minimum in spring and after the minimum in autumn were removed (i.e., the ones beyond the phenology

thresholds in Fig. S3). The smoother was then used to determine $D1_{NDVI}$, i.e., the date at which the fitted NDVI crosses a threshold value of 0 (before reaching the yearly maximum), and to determine A_{NDVI}, i.e., the area underneath the smoother from the start ($D1_{NDVI}$) to the end ($D2_{NDVI}$) of the season (with the latter defined as the date at which the fitted NDVI crosses a threshold value of 0.1, after having reached the yearly maximum). A threshold of 0.1 was used for defining $D2_{NDVI}$ since the vegetation index was in general still above 0 at the start of the snow-covered season. An example of the latter procedure is given in Fig. S3, with all estimates listed in Table S1. Note that data are missing for the second half of 1994. The R code used to extract these indices from the raw data on temperature, snow cover, and NDVI can be found at Dryad at http://dx.doi.org/10.5061/dryad.n1m8d.

Body size of juvenile red knots at first stopover (Poland)

Every autumn, between 1983 and 2015, we captured red knots at a stopover site in Poland, Gdańsk Bay (*38-39*), a site that is mainly used by juvenile red knots (after having left the breeding grounds, adult red knots, which migrate earlier and separately from juvenile birds, usually make their first stopover in the Wadden Sea (*40*)). Birds were captured in walk-in traps, where after they were aged on the basis of plumage (*41*), distinguishing juveniles (1st-calendar-year birds) from adults (> 2nd-calendar-year), and body mass (± 1 g) and structural size measurements were recorded, including length of bill (± 0.1 mm), tarsus (± 0.1 mm) and wing (± 1 mm). Using these three structural measures, overall body size was calculated as the first principle component (PC1) in a PCA analysis (*pca* function from R package *pcaMethods*, which enables imputation of missing values if at least one of three measures was taken). Body size metrics were related to Taimyr climatic data using mixed-effect modeling, including year as a random-intercept effect (*lme* function from R package *nlme*). Model selection was based on comparison of Akaike's information criterion adjusted for small sample size (AIC_c) (*42*). To make models comparable, 1994 was excluded from all models since A_{NDVI} could not be estimated for that year. Across the entire 33-year period, a total of 2,760 red knots were caught, including 1,990 juveniles (only in 1987 were no juveniles caught). After removing the year 1994 and those birds that were not measured biometrically, this left 1,820 juveniles for analysis (of which bill length was measured in 1,808 birds and body mass in 1,764 birds). Years with fewer than 10 knots caught are excluded in Figs. 2BC (but not in the mixed-effect modeling).

Body size, diet and survival of red knots at their wintering site (Mauritania)

In Banc d'Arguin (Mauritania) we caught a total of 2,508 red knots across 12 winters (2002-2013) from November to January. Catches were mostly done by using mist-nets, except for one catch for which we used canon-nets (January 2013). Upon capture, the birds were aged as juvenile (1st winter) or adult (>1st winter) based on their plumage (*41*). Furthermore, body mass (± 1 g) and structural size measurements were recorded, including length of bill (± 0.1 mm), tarsus (± 0.1 mm) and wing (± 1

mm). These three structural measures formed the input for a PCA in order to express overall body size as PC1, the latter which was analyzed for changes over time using the *lm* function in R.

From the brachial vein a small blood sample (10-100 µL) was taken, which was stored in 70% ethanol. At NIOZ, samples were stored at -80 ºC until analysis. After extracting DNA to molecularly identify each individual's sex (*43*), leftovers of the samples were used to determine the stable isotope ratios of carbon (^{13}C) and nitrogen (^{15}N). In order to do so, samples were freeze-dried to constant mass (*44*) before analysis in a Thermo Scientific (Flash 2000) organic element analyzer coupled to a Delta V isotope ratio mass spectrometer. A microbalance (Sartorius XM1000P) was used to weigh 0.4-0.8 mg of freeze-dried blood into 5 x 9 mm tin capsules. Isotope values were calibrated to an acetanilide lab standard, controlled for a urea lab standard and corrected for blank tin capsules. In this way we were able to analyze blood samples of most birds (i.e., 2,340 individuals), which we analyzed in random order with respect to year. Stable isotope ratios of the three main food sources (*Dosinia isocardia*, *Loripes lucinalis* and rhizomes of *Zostera noltii*) were taken from Catry *et al*. (*45*), and the discrimination values from an experimental validation study, in which captive red knots were given a monospecific diet consisting either of *Dosinia* or *Loripes (46)*. Discrimination values for *Zostera* are unknown for which we took the average across *Dosinia* and *Loripes*. These values were then used by the *siarsolomcmcv4* function from the R package *siar* (*47*) to estimate the relative contribution of each food source to an individual's diet.

Before release, birds were tagged using a combination of four color-bands and a flag, allowing individual recognition in the field, thereby enabling annual survival rate estimations (*15, 48-49*). By intense resighting efforts using telescopes in subsequent 12 nonbreeding seasons, in addition to 48 physical recaptures, we could estimate annual winter-to-winter survival rate across the 12 intervening years (i.e., for 2,508 –127 = 2,381 birds caught in the first 12 nonbreeding seasons; 127 birds were excluded as they participated in laboratory or field experiments). The majority of resightings (88%) were performed in winter (Oct-Feb) in our study area in Banc d'Arguin, 10% of the resightings were performed during autumn and spring migration in Banc d'Arguin, and 2% were performed elsewhere along the flyway, mainly in the Wadden Sea area in The Netherlands and Germany (for the distribution of these resightings over the years, see Table S5). As the vast majority of resightings (79%) were performed in November and December, survival is roughly estimated from December in year *i* to November in year *i*+1. We used mark-recapture modelling and Cormack-Jolly-Seber models to separate apparent survival (Φ) (hereafter survival) from resighting probabilities (p) – apparent survival because mortality is confounded with permanent emigration (*18*). However, we have no evidence for emigration. Observers well aware of the individual marking program neither noticed a single marked bird from our study population in the rest of the Banc d'Arguin outside our study area, nor in the Archipelago dos Bijagos in Guinea-Bissau, where the remaining part of the population is wintering (ca. 20%). As there were indications of ring-reading errors (for methods, see (*50*)), we considered an individual as resighted during a particular nonbreeding season only when it

was seen at least twice during that season. Building upon previous findings (*15, 48-49*), we included the following explanatory variables in all models: time (t), age (a, distinguishing juveniles and adults) and time-since-marking effects (tsm) on survival, and time and site (s) effects on resighting probability (ringing and resighting efforts were performed at two demographically distinct sites in Banc d'Arguin: Baie d'Aouatif and Abelgh Eiznaya (*48*)). Our most parameterized 'full' model was $\Phi_{tsm \cdot t+a \cdot t}\ p_{t \cdot s}$ for which the median ĉ test implemented in program MARK (*51*) indicated no significant overdispersion (ĉ =1.03 ± 0.004).

Model selection was performed in two steps. In step 1, we considered biologically meaningful reductions of the full model (i.e., by removing interactions between the above-mentioned explanatory variables) without considering covariates yet and in step 2, we used the best-supported model from step 1 to assess support for survival being a function of bill length for either or both juveniles and adults. In addition, we considered models in which juvenile survival was constrained to be a function of date of snowmelt in their year of birth, or of year of birth (as a continuous variable), while adult survival was allowed to vary between years. We calculated the $R^2_{dev} = \frac{Dev_{cst} - Dev_{snow}}{Dev_{cst} - Dev_t}$ to reflect the proportion of temporal variation in juvenile survival that was explained by variation in the date of snowmelt (*52*).

Model selection was performed on the basis of the Akaike information criterion corrected for small sample size AIC_c (*42*) where a model was considered as better supported than other models when its AIC_c was at least two points lower. Models were constructed in program R using package *RMark* (*53*) and run using the optimization algorithm of program MARK v. 8.0 (*51*).

<u>Depth distribution of the red knots' wintering food supply (Mauritania)</u>

Depth distributions for *Loripes* and *Dosinia* were taken from the literature (*54*), which we corrected for the length distribution that we found in our benthos samples over the study period 2002-2013 (*15*), by fitting linear regressions through the published depth-length graphs (*54*). The depth distribution of *Zostera* rhizomes was measured at 8 sites throughout our study area in January 2013, with 4 repeated measures per site at a precision of 1 mm using a ruler. Depth distributions are expressed on the basis of individual numbers, not on the basis of biomass.

Supplementary Materials: Figures

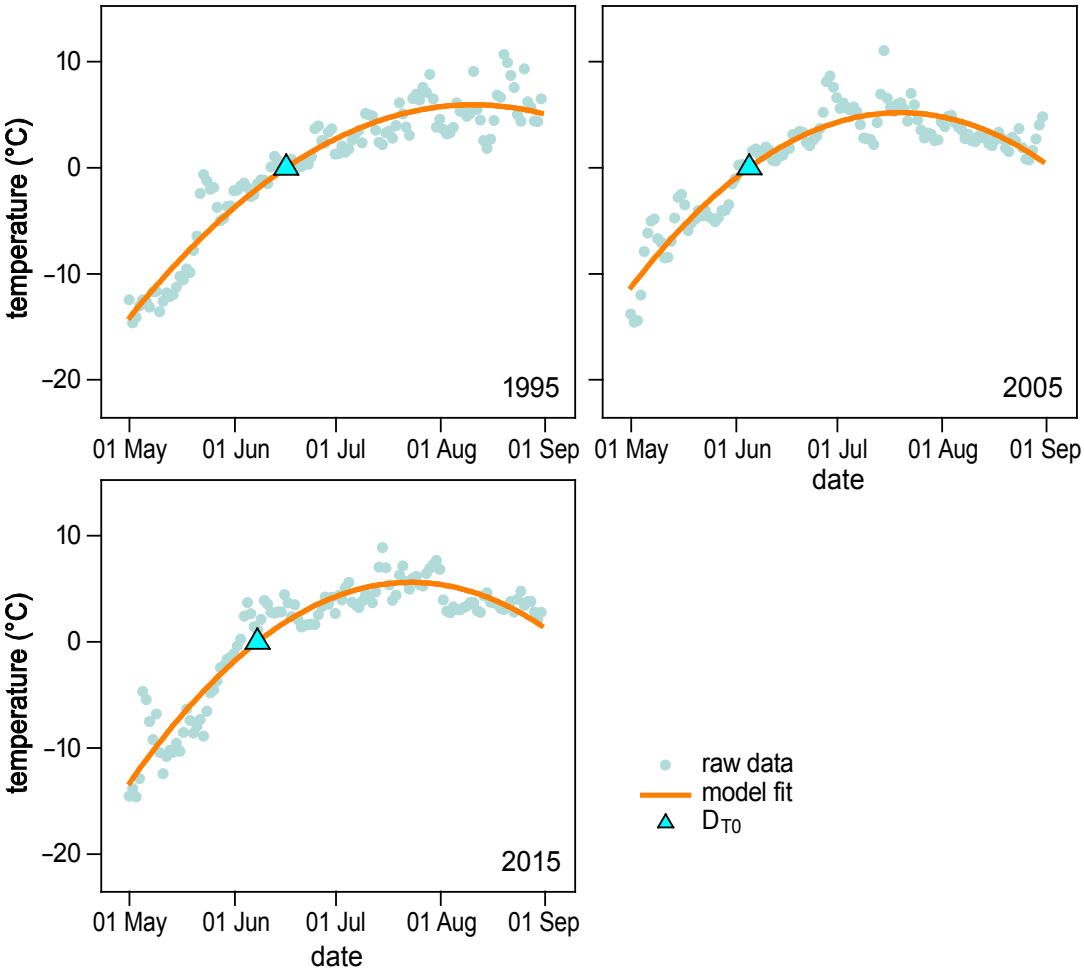

Fig. S1. Estimating D_{T0} exemplified for three different years. The date D_{T0} at which ambient temperature exceeded 0 °C for the first time of year was found by fitting a quadratic regression (orange line) through daily mean temperatures (grey dots). Annual estimates for D_{T0} are listed in Table S1.

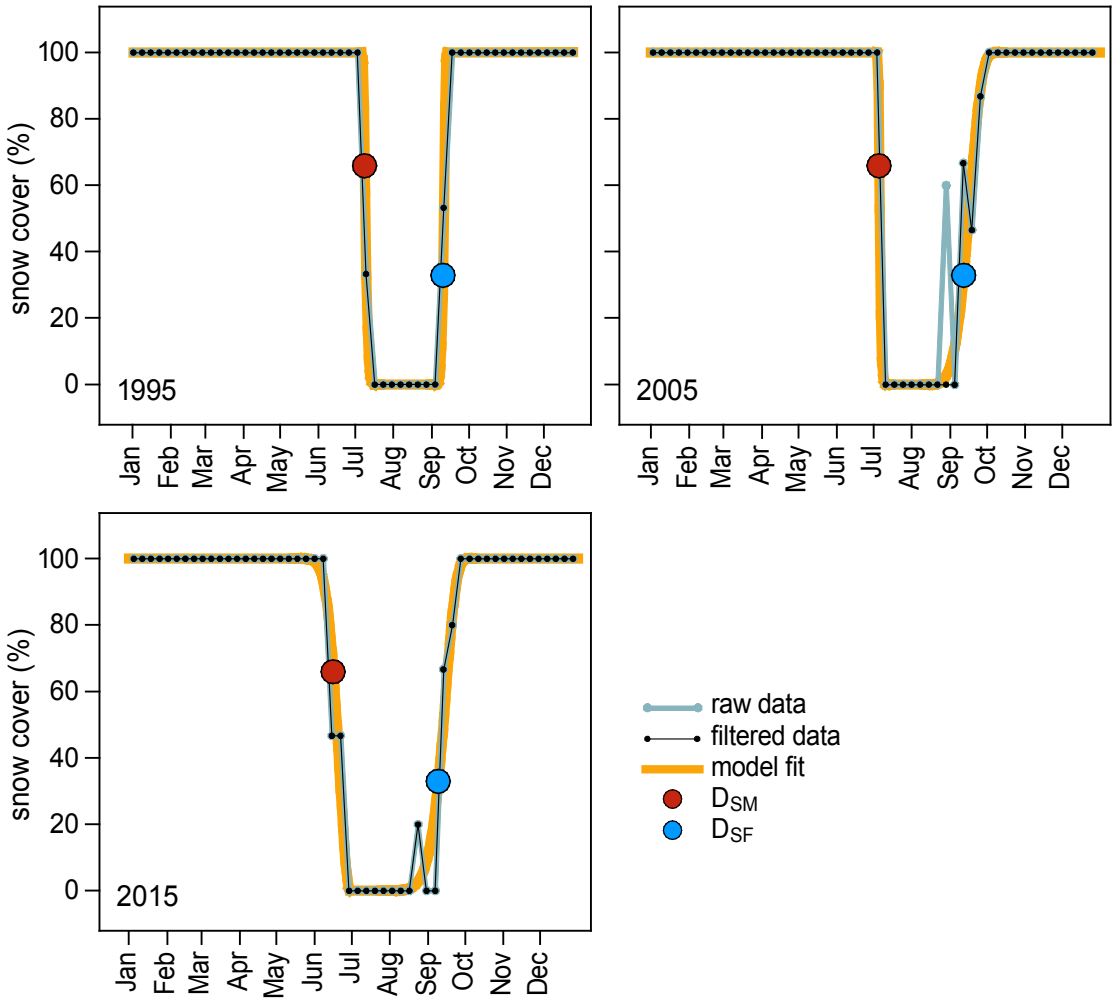

Fig. S2. Estimating D_{SM} and D_{SF} exemplified for three different years. Date of snowmelt D_{SM} and date of snowfall D_{SF} were found by fitting an asymmetric Gaussian model (orange line) through filtered (black dots) weekly estimates of snow cover (grey dots). D_{SM} and D_{SF} are listed for each year in Table S1.

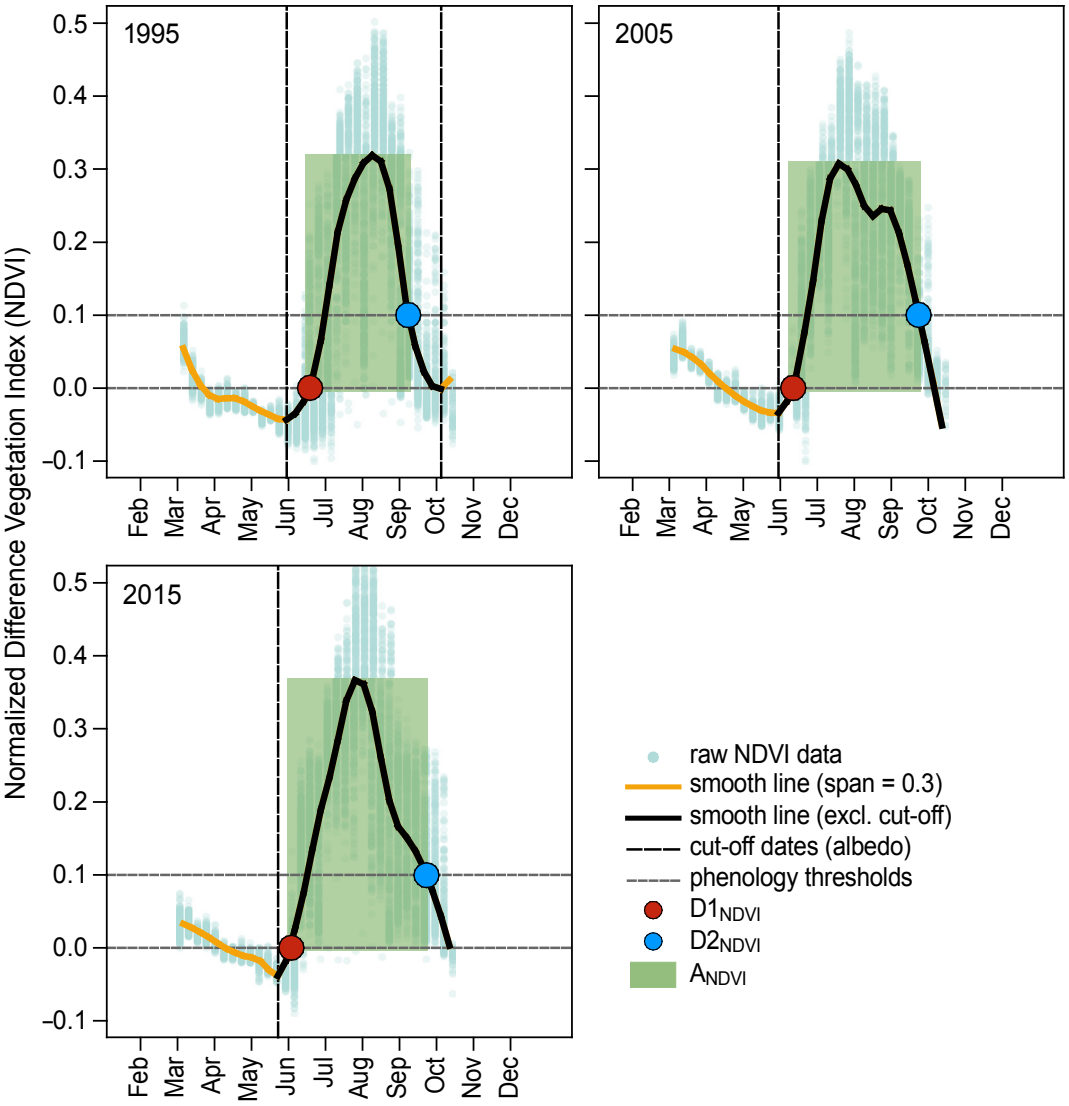

Fig. S3. Estimating $D1_{NDVI}$, $D2_{NDVI}$, and A_{NDVI} exemplified for three different years. By fitting a smoother (orange and black line) through weekly raw NDVI data, we estimated the beginning ($D1_{NDVI}$) and the end ($D2_{NDVI}$) of the 'greening' season, and the overall intensity, the latter represented by A_{NDVI}, the area underneath the smoother between $D1_{NDVI}$ and $D2_{NDVI}$. Annual estimates for $D1_{NDVI}$, $D2_{NDVI}$, and A_{NDVI} are listed in Table S1.

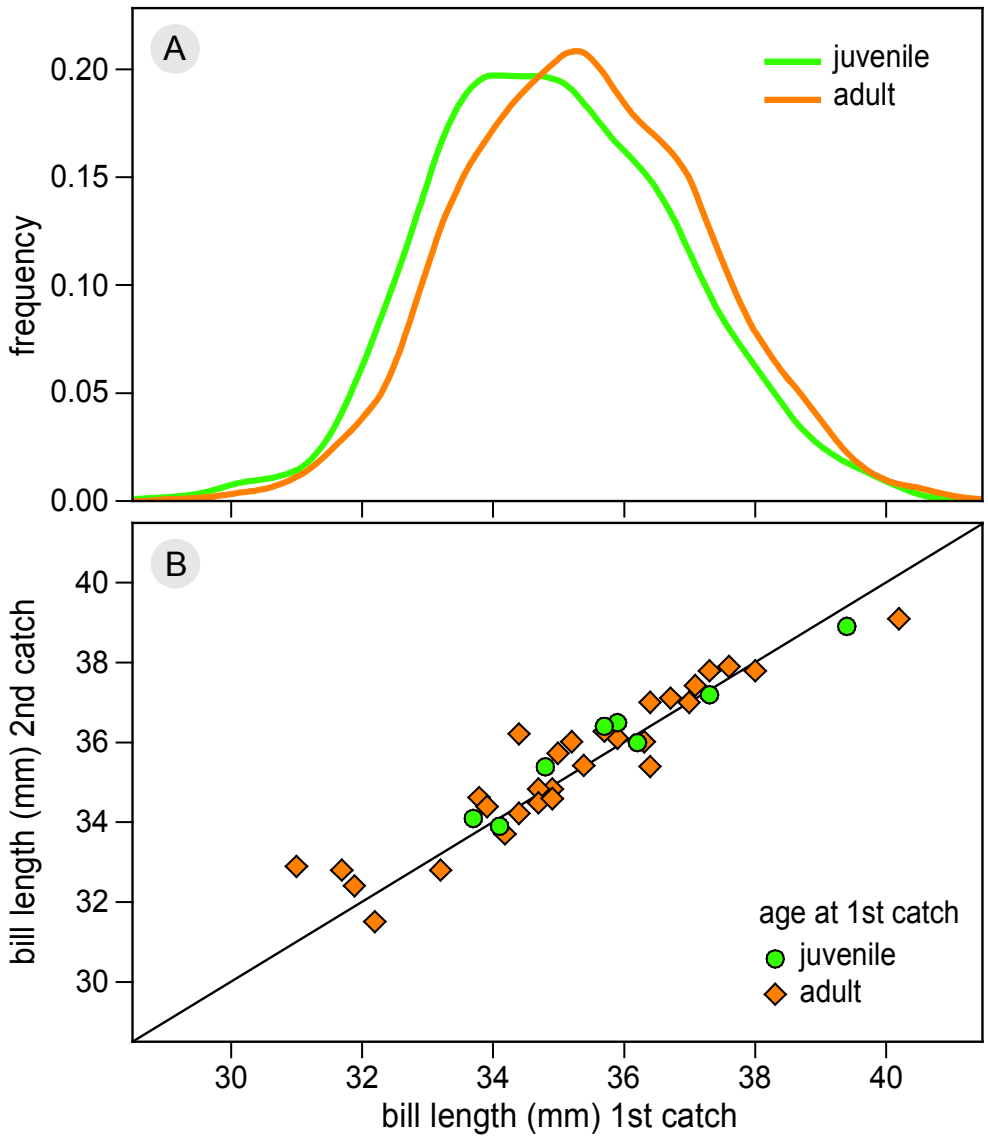

Fig. S4. Bill lengths in Banc d'Arguin from 2002 to 2013. (A) Frequency distributions of bill lengths in Banc d'Arguin for juveniles (n = 717 birds) and adults (n = 1,791 birds), showing that juveniles have on average shorter bills than adults. (B) Upon their first arrival in the tropics, red knots maintain a constant bill length for the rest of their life, as shown in individuals that were retrapped as adult (y-axis) but initially caught as juvenile or adult (x-axis) (n = 37 birds, R^2= .89, $F_{1,35}$ = 297.8, P < .00001; interval between first and second catch ranges from 1-11 years). Hence, the absence of bill growth at the nonbreeding grounds supports the idea that juveniles generally have shorter bills than adults due to selective mortality.

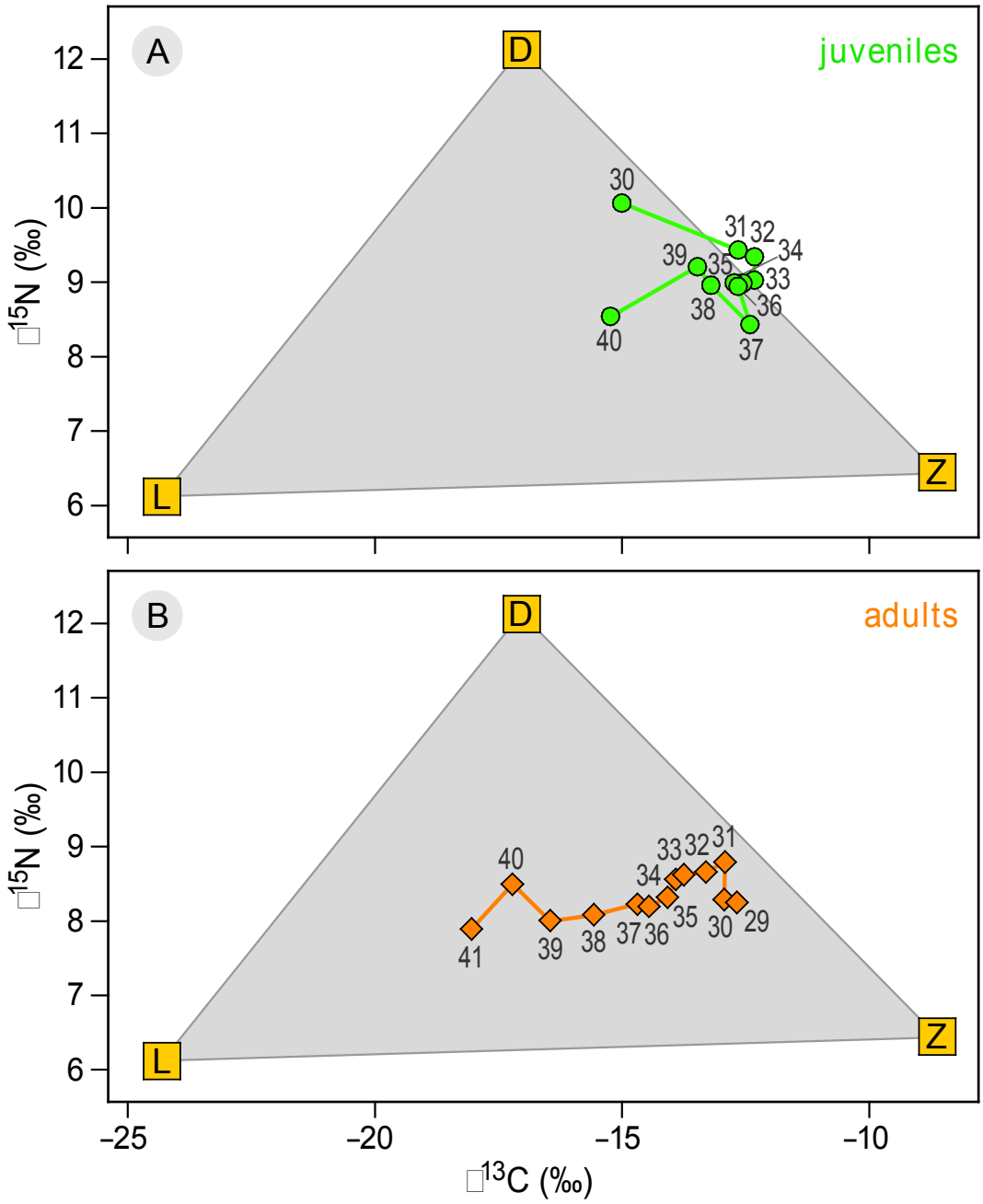

Fig. S5. Stable-isotope ratios of red knots in Banc d'Arguin from 2002 to 2013. Data are averaged per 1-mm bill length class given by number next to each symbol, and are plotted separately for juveniles (A; *n* = 676 birds) and adults (B; *n* = 1,664 birds) in relation to discrimination-corrected values in the food (*D* denotes *Dosinia isocardia*, *L* denotes *Loripes lucinalis* and *Z* denotes *Zostera noltii*).

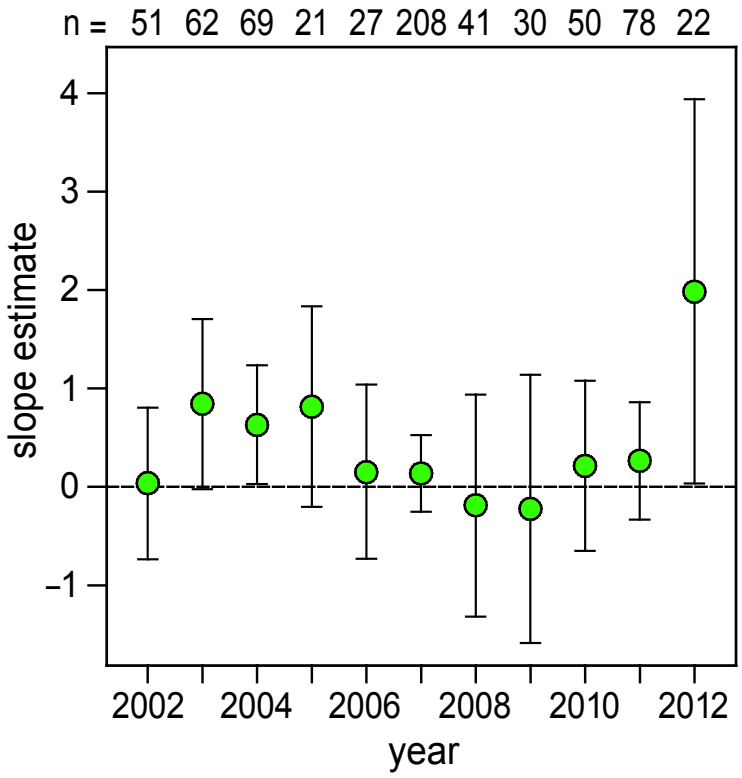

Fig. S6. Birth year-specific estimates of the slope between bill length (in mm) and juvenile survival (on a logit scale). Estimates are from the model $\Phi_{tsm \cdot t+a+juv \cdot bill \cdot t}\ p_{s+t}$ (model 10, Table S7). Sample sizes of juvenile birds are shown at the top of the graph. The slope was estimated to be positive in 9 out of 11 years, and significantly so (with the 95% confidence interval, indicated by the error bar, not including zero) in two years (2004 and 2012).

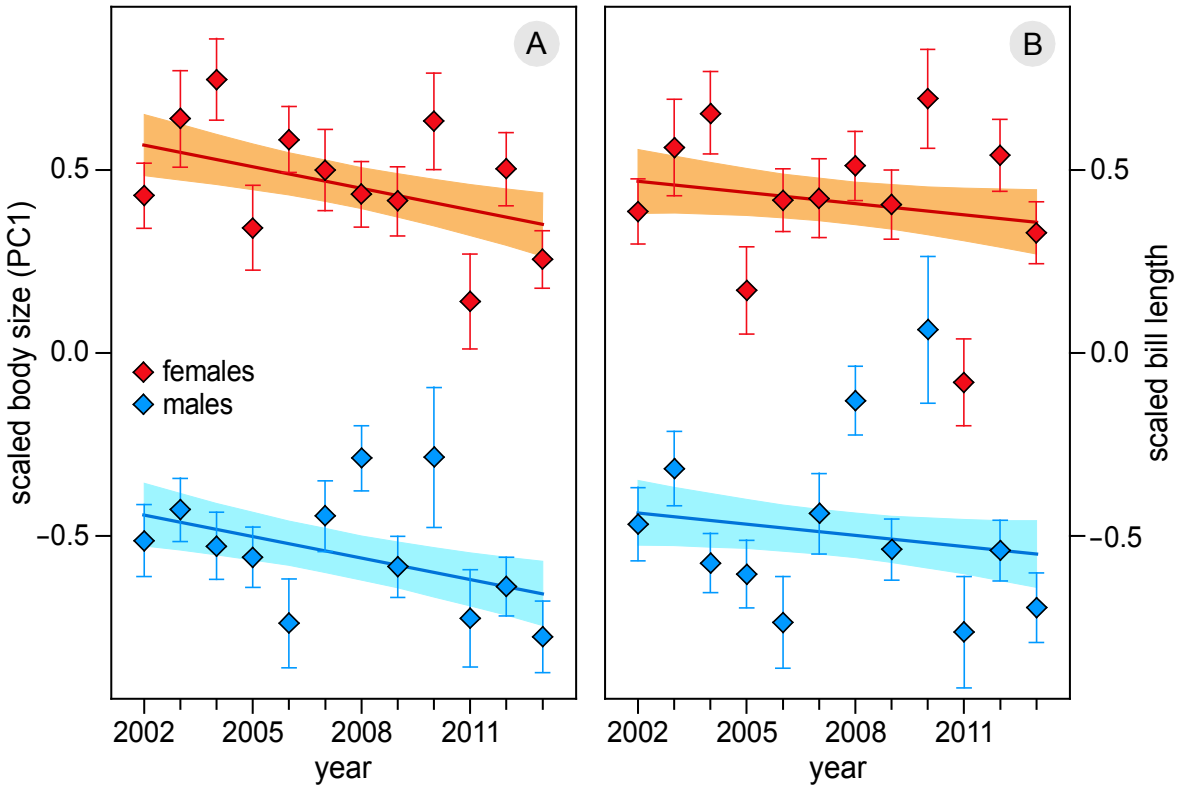

Fig. S7. Changes in overall body size and bill length in adult red knots caught in Mauritania 2002-2013. (A) First principle component (PC1), including bill length (loading 0.65), tarsus length (loading 0.58), and wing length (loading 0.49), decreased at a rate of 0.020 SD year^{-1}, in both females and males (R^2 = .26, $F_{2,1727}$ = 299.20, P < .001; slopes did not differ between sexes, P = 0.65). (B) Over the same period bill length alone decreased at a rate of only 0.010 SD year^{-1} in both females and males (R^2 = .21, $F_{2,1727}$ = 223.57, P = .097; slopes did not differ between sexes, P = 0.94). Analysis includes 1,730 out of 1,791 adults for which sex could be determined.

Supplementary Materials: Tables

Table S1. Climate phenology parameters in the red knot's breeding range at Taimyr Peninsula. Given are the date at which ambient temperature exceeds 0 °C (D_{T0}; Fig. S1); date of snowmelt (D_{SM}) and snowfall (D_{SF}; Fig. S2); date at which NDVI exceeds ($D1_{NDVI}$) and falls below ($D2_{NDVI}$) a threshold value, and the surface area underneath the NDVI smoother (A_{NDVI}; Fig. S3).

Year	D_{T0}	D_{SM}	D_{SF}	$D1_{NDVI}$	$D2_{NDVI}$	A_{NDVI}
1983	23-Jun	04-Jul	20-Sep	20-Jun	25-Sep	16.76
1984	17-Jun	02-Jul	06-Oct	16-Jun	22-Sep	25.73
1985	17-Jun	15-Jul	27-Sep	07-Jun	07-Sep	21.01
1986	20-Jun	13-Jul	19-Sep	30-Jun	12-Sep	20.84
1987	24-Jun	14-Jul	14-Sep	03-Jul	25-Sep	15.96
1988	18-Jun	29-Jun	04-Sep	16-Jun	10-Sep	17.38
1989	30-Jun	23-Jul	13-Sep	08-Jul	07-Sep	7.32
1990	14-Jun	30-Jun	31-Aug	19-Jun	02-Oct	20.99
1991	16-Jun	01-Jul	04-Oct	27-Jun	01-Oct	20.98
1992	28-Jun	07-Jul	29-Aug	28-Jun	11-Sep	14.50
1993	18-Jun	27-Jun	02-Sep	17-Jun	21-Sep	16.36
1994	20-Jun	07-Jul	14-Sep	19-Jun	-	-
1995	16-Jun	08-Jul	10-Sep	19-Jun	08-Sep	19.03
1996	20-Jun	13-Jul	26-Aug	06-Jul	22-Sep	16.96
1997	14-Jun	02-Jul	13-Sep	25-Jun	20-Sep	19.28
1998	12-Jun	11-Jul	19-Sep	19-Jun	16-Sep	23.63
1999	09-Jun	22-Jun	20-Sep	13-Jun	26-Sep	19.13
2000	11-Jun	14-Jul	10-Sep	27-Jun	10-Sep	19.48
2001	08-Jun	18-Jun	20-Sep	15-Jun	27-Sep	30.51
2002	10-Jun	30-Jun	14-Sep	22-Jun	18-Sep	20.76
2003	09-Jun	08-Jul	23-Sep	16-Jun	29-Sep	21.11
2004	12-Jun	06-Jul	19-Sep	27-Jun	17-Sep	23.26
2005	04-Jun	05-Jul	12-Sep	12-Jun	24-Sep	23.66
2006	06-Jun	03-Jul	08-Sep	16-Jun	17-Sep	22.12
2007	09-Jun	25-Jun	14-Sep	23-Jun	04-Oct	24.11
2008	13-Jun	04-Jul	14-Sep	25-Jun	28-Sep	19.40
2009	07-Jun	29-Jun	02-Oct	19-Jun	04-Oct	20.59
2010	05-Jun	17-Jun	12-Sep	14-Jun	20-Sep	18.88
2011	01-Jun	17-Jun	21-Sep	03-Jun	29-Sep	27.65
2012	05-Jun	13-Jun	30-Sep	02-Jun	29-Sep	33.61
2013	12-Jun	05-Jul	22-Sep	16-Jun	26-Sep	24.47
2014	07-Jun	26-Jun	03-Sep	21-Jun	16-Sep	18.16
2015	07-Jun	16-Jun	09-Sep	06-Jun	26-Sep	25.43

Table S2. Models relating juvenile body mass at the Polish stopover site to annual climatic conditions at Taimyr Peninsula. Climate parameters tested for are date of snowmelt (D_{SM}), date of snowfall (D_{SF}), date at which temperature > 0 ºC (D_{T0}), date at which NDVI crossed a threshold ($D1_{NDVI}$), and area under the NDVI curve (A_{NDVI}). Analysis includes 1,764 birds caught in 31 years. Models are sorted by AIC_c, with the most parsimonious model given in bold (i.e., model having the fewest parameters K among models which $\Delta AIC_c < 2$).

Model	K	AIC_c	ΔAIC_c	AIC_cWt	Cum.Wt	LL
$\sim D_{T0}+A_{NDVI}$	5	14765.93	0.00	0.14	0.14	-7377.95
$\sim D_{T0}+D_{SF}$	5	14766.17	0.24	0.13	0.27	-7378.07
$\sim D_{T0}+D_{SM}+A_{NDVI}$	6	14766.39	0.46	0.11	0.38	-7377.17
$\sim D_{T0}+D_{SF}+A_{NDVI}$	6	14766.82	0.89	0.09	0.48	-7377.39
$\sim D_{T0}$	**4**	**14767.02**	**1.09**	**0.08**	**0.56**	**-7379.50**
$\sim D_{T0}+D_{SM}+D_{SF}+A_{NDVI}$	7	14767.70	1.77	0.06	0.62	-7376.82
$\sim D_{T0}+D1_{NDVI}+A_{NDVI}$	6	14767.73	1.81	0.06	0.68	-7377.84
$\sim D_{T0}+D_{SM}+D_{SF}$	6	14767.74	1.81	0.06	0.73	-7377.84
$\sim D_{T0}+D_{SF}+D1_{NDVI}$	6	14768.17	2.24	0.05	0.78	-7378.06
$\sim D_{T0}+D_{SM}+D1_{NDVI}+A_{NDVI}$	7	14768.40	2.48	0.04	0.82	-7377.17
$\sim D_{T0}+D_{SM}$	5	14768.43	2.51	0.04	0.86	-7379.20
$\sim D_{T0}+D_{SF}+D1_{NDVI}+A_{NDVI}$	7	14768.55	2.62	0.04	0.90	-7377.24
$\sim D_{T0}+D1_{NDVI}$	5	14768.97	3.04	0.03	0.93	-7379.47
$\sim D_{T0}+D_{SM}+D_{SF}+D1_{NDVI}+A_{NDVI}$	8	14769.69	3.77	0.02	0.96	-7376.81
$\sim D_{T0}+D_{SM}+D_{SF}+D1_{NDVI}$	7	14769.72	3.80	0.02	0.98	-7377.83
$\sim D_{T0}+D_{SM}+D1_{NDVI}$	6	14770.06	4.13	0.02	1.00	-7379.01
$\sim D_{SM}$	4	14775.24	9.31	0.00	1.00	-7383.61
$\sim D_{SM}+D_{SF}$	5	14776.74	10.81	0.00	1.00	-7383.35
$\sim D_{SM}+D1_{NDVI}$	5	14777.10	11.18	0.00	1.00	-7383.54
$\sim D_{SM}+A_{NDVI}$	5	14777.21	11.28	0.00	1.00	-7383.59
$\sim D_{SM}+D_{SF}+D1_{NDVI}$	6	14778.31	12.38	0.00	1.00	-7383.13
$\sim D_{SM}+D_{SF}+A_{NDVI}$	6	14778.72	12.79	0.00	1.00	-7383.34
$\sim D_{SM}+D1_{NDVI}+A_{NDVI}$	6	14778.96	13.03	0.00	1.00	-7383.45
$\sim D_{SM}+D_{SF}+D1_{NDVI}+A_{NDVI}$	7	14780.32	14.40	0.00	1.00	-7383.13
$\sim D1_{NDVI}$	4	14780.84	14.91	0.00	1.00	-7386.41
$\sim D_{SF}+D1_{NDVI}$	5	14781.54	15.61	0.00	1.00	-7385.75
$\sim D1_{NDVI}+A_{NDVI}$	5	14782.75	16.82	0.00	1.00	-7386.36
$\sim D_{SF}+D1_{NDVI}+A_{NDVI}$	6	14782.88	16.95	0.00	1.00	-7385.41
$\sim A_{NDVI}$	4	14783.70	17.77	0.00	1.00	-7387.84
$\sim A_{NDVI}+D_{SF}$	5	14784.10	18.17	0.00	1.00	-7387.03
$\sim D_{SF}$	4	14786.98	21.05	0.00	1.00	-7389.48

Table S3. Models relating juvenile bill length at the Polish stopover site to annual climatic conditions at Taimyr Peninsula. Analysis includes 1,808 birds caught in 31 years.

Model	K	AIC_c	ΔAIC_c	$AIC_c Wt$	Cum.Wt	LL
$\sim D_{T0}+D_{SM}+D1_{NDVI}+A_{NDVI}$	7	7609.74	0.00	0.19	0.19	-3797.84
$\sim D_{SM}+D1_{NDVI}+A_{NDVI}$	6	7610.44	0.70	0.13	0.32	-3799.20
$\sim D_{SM}+A_{NDVI}$	**5**	**7610.48**	**0.74**	**0.13**	**0.46**	**3800.22**
$\sim D_{T0}+D_{SM}+A_{NDVI}$	6	7610.77	1.03	0.11	0.57	-3799.36
$\sim D_{T0}+D_{SM}+D_{SF}+D1_{NDVI}+A_{NDVI}$	8	7610.91	1.17	0.11	0.68	-3797.41
$\sim D_{SM}+D_{SF}+D1_{NDVI}+A_{NDVI}$	7	7611.73	1.99	0.07	0.75	-3798.83
$\sim D_{SM}+D_{SF}+A_{NDVI}$	6	7612.07	2.33	0.06	0.81	-3800.01
$\sim D_{T0}+D_{SM}+D_{SF}+A_{NDVI}$	7	7612.33	2.59	0.05	0.86	-3799.14
$\sim D_{T0}+A_{NDVI}$	5	7613.35	3.61	0.03	0.89	-3801.66
$\sim D_{SM}+D1_{NDVI}$	5	7613.81	4.08	0.02	0.91	-3801.89
$\sim D_{T0}+D1_{NDVI}+A_{NDVI}$	6	7614.83	5.09	0.01	0.93	-3801.39
$\sim D_{T0}+D_{SF}+A_{NDVI}$	6	7615.33	5.59	0.01	0.94	-3801.64
$\sim D_{T0}+D_{SM}+D1_{NDVI}$	6	7615.43	5.69	0.01	0.95	-3801.69
$\sim D_{SM}+D_{SF}+D1_{NDVI}$	6	7615.76	6.02	0.01	0.96	-3801.85
$\sim D_{T0}+D_{SF}+D1_{NDVI}+A_{NDVI}$	7	7616.79	7.05	0.01	0.97	-3801.37
$\sim D_{SM}$	4	7616.89	7.15	0.01	0.97	-3804.43
$\sim D_{T0}+D_{SM}+D_{SF}+D1_{NDVI}$	7	7617.32	7.58	0.00	0.98	-3801.63
$\sim D_{T0}+D1_{NDVI}$	5	7617.87	8.13	0.00	0.98	-3803.92
$\sim D_{SM}+D_{SF}$	5	7618.10	8.36	0.00	0.98	-3804.03
$\sim D_{T0}$	4	7618.23	8.50	0.00	0.98	-3805.11
$\sim A_{NDVI}$	4	7618.40	8.66	0.00	0.99	-3805.19
$\sim D_{T0}+D_{SM}$	5	7618.88	9.15	0.00	0.99	-3804.43
$\sim D_{SF}$	4	7619.01	9.27	0.00	0.99	-3805.50
$\sim D1_{NDVI}$	4	7619.28	9.54	0.00	0.99	-3805.63
$\sim D_{T0}+D_{SF}$	5	7619.34	9.60	0.00	0.99	-3804.65
$\sim D_{T0}+D_{SF}+D1_{NDVI}$	6	7619.44	9.70	0.00	1.00	-3803.70
$\sim D_{T0}+D_{SM}+D_{SF}$	6	7620.10	10.36	0.00	1.00	-3804.03
$\sim D1_{NDVI}+A_{NDVI}$	5	7620.24	10.50	0.00	1.00	-3805.10
$\sim D_{SF}+A_{NDVI}$	5	7620.37	10.64	0.00	1.00	-3805.17
$\sim D_{SF}+D1_{NDVI}$	5	7620.99	11.25	0.00	1.00	-3805.48
$\sim D_{SF}+D1_{NDVI}+A_{NDVI}$	6	7622.22	12.48	0.00	1.00	-3805.09

Table S4. Models relating overall juvenile body size at the Polish stopover site to annual climatic conditions at Taimyr Peninsula. Overall body size is expressed as PC1 from a principal component analysis including bill length (loading 0.66), tarsus length (loading 0.42), and wing length (loading 0.63). Analysis includes 1,820 birds caught in 31 years.

Model	K	AIC_c	ΔAIC_c	AIC_cWt	Cum.Wt	LL
$\sim D_{SM}+A_{NDVI}$	**5**	**5925.22**	**0.00**	**0.16**	**0.16**	**-2957.59**
$\sim D_{T0}+A_{NDVI}$	5	5925.95	0.73	0.11	0.26	-2957.96
$\sim D_{T0}+D_{SM}+A_{NDVI}$	6	5926.41	1.19	0.09	0.35	-2957.18
$\sim D_{SM}+D_{SF}+A_{NDVI}$	6	5926.77	1.55	0.07	0.42	-2957.36
$\sim D_{SM}+D1_{NDVI}+A_{NDVI}$	6	5926.79	1.57	0.07	0.49	-2957.37
$\sim A_{NDVI}$	4	5927.39	2.18	0.05	0.54	-2959.69
$\sim D_{T0}+D_{SM}+D1_{NDVI}+A_{NDVI}$	7	5927.73	2.51	0.04	0.59	-2956.83
$\sim D_{T0}+D_{SF}+A_{NDVI}$	6	5927.81	2.60	0.04	0.63	-2957.88
$\sim D_{T0}+D1_{NDVI}+A_{NDVI}$	6	5927.84	2.62	0.04	0.67	-2957.90
$\sim D_{T0}+D_{SM}+D_{SF}+A_{NDVI}$	7	5927.96	2.74	0.04	0.71	-2956.95
$\sim D_{SM}+D_{SF}+D1_{NDVI}+A_{NDVI}$	7	5928.20	2.99	0.03	0.75	-2957.07
$\sim D_{T0}+D_{SM}+D_{SF}+D1_{NDVI}+A_{NDVI}$	8	5929.09	3.88	0.02	0.77	-2956.51
$\sim D_{SM}+D1_{NDVI}$	5	5929.23	4.02	0.02	0.79	-2959.60
$\sim D1_{NDVI}$	4	5929.24	4.02	0.02	0.81	-2960.61
$\sim D1_{NDVI}+A_{NDVI}$	5	5929.25	4.03	0.02	0.83	-2959.61
$\sim D_{SF}$	4	5929.38	4.16	0.02	0.85	-2960.68
$\sim D_{SF}+A_{NDVI}$	5	5929.39	4.18	0.02	0.87	-2959.68
$\sim D_{SM}$	4	5929.54	4.32	0.02	0.89	-2960.76
$\sim D_{T0}+D_{SF}+D1_{NDVI}+A_{NDVI}$	7	5929.69	4.47	0.02	0.91	-2957.82
$\sim D_{T0}$	4	5929.72	4.50	0.02	0.92	-2960.85
$\sim D_{T0}+D1_{NDVI}$	5	5930.29	5.08	0.01	0.93	-2960.13
$\sim D_{SM}+D_{SF}$	5	5931.06	5.84	0.01	0.94	-2960.51
$\sim D_{SF}+D1_{NDVI}$	5	5931.07	5.85	0.01	0.95	-2960.52
$\sim D_{T0}+D_{SM}+D1_{NDVI}$	6	5931.17	5.95	0.01	0.96	-2959.56
$\sim D_{SM}+D_{SF}+D1_{NDVI}$	6	5931.18	5.97	0.01	0.97	-2959.57
$\sim D_{T0}+D_{SF}$	5	5931.23	6.02	0.01	0.97	-2960.60
$\sim D_{SF}+D1_{NDVI}+A_{NDVI}$	6	5931.25	6.03	0.01	0.98	-2959.60
$\sim D_{T0}+D_{SM}$	5	5931.51	6.30	0.01	0.99	-2960.74
$\sim D_{T0}+D_{SF}+D1_{NDVI}$	6	5932.09	6.87	0.01	0.99	-2960.02
$\sim D_{T0}+D_{SM}+D_{SF}$	6	5933.07	7.85	0.00	1.00	-2960.51
$\sim D_{T0}+D_{SM}+D_{SF}+D1_{NDVI}$	7	5933.10	7.88	0.00	1.00	-2959.52

Table S5. Number of resighted color-banded red knots per year. Listed are individuals that were resighted at least twice during the winter period (Oct-Mar) in Banc d'Arguin, the migratory periods in Banc d'Arguin (Aug-Sep and Apr-May), and elsewhere along the flyway (with most resightings performed during autumn and spring migration in the Wadden Sea area in The Netherlands and Germany). 2002 refers to the period July 2002 to June 2003.

Year	Banc d'Arguin (winter)	Banc d'Arguin (migration)	Europe
2002	25	0	1
2003	41	0	1
2004	64	79	7
2005	146	0	6
2006	200	119	9
2007	242	43	12
2008	191	58	10
2009	306	0	4
2010	259	0	0
2011	281	0	3
2012	169	0	1
2013	336	0	3
2014	367	0	5

Table S6. Model selection results of step 1 of the survival analysis.

Model	K	ΔDeviance	ΔAIC_c	Akaike weight
(1) $\Phi_{tsm \cdot t + a}\, p_{s+t}$	37	19.22	0.00*	0.99
(2) $\Phi_{tsm \cdot t + a}\, p_{s \cdot t}$	47	7.74	8.90	0.01
(3) $\Phi_{tsm + t + a}\, p_{s+t}$	26	53.97	12.44	0.00
(4) $\Phi_{tsm \cdot t + a \cdot t}\, p_{s+t}$	48	11.40	14.60	0.00
(5) $\Phi_{tsm + t + a}\, p_{s \cdot t}$	37	38.43	19.20	0.00
(6) $\Phi_{tsm + a \cdot t}\, p_{s+t}$	37	41.54	22.32	0.00
(7) $\Phi_{tsm \cdot t + a \cdot t}\, p_{s \cdot t}$	58	0.00**	23.68	0.00
(8) $\Phi_{tsm + a \cdot t}\, p_{s \cdot t}$	47	27.82	28.98	0.00

*AIC_c = 11749.78

**Deviance = 2411.89

tsm=time-since-marking (first year after marking modelled separately from later years); t=time (years); a=age, distinguishing first-year (juvenile) and older (adult) birds; s=site. An interaction between effects is denoted by '·', whereas additive effects are denoted by '+'. Note that an interaction between age and time-since-marking is not possible, because juvenile survival can only be estimated in the first year after marking.

Table S7. Model selection results of step 2 of the survival analysis. In all models, resighting probability is modelled as the most parsimonious parameterization from step 1: p_{s+t}.

Model	K	ΔDeviance	ΔAIC_c	Akaike weight
(1) $\Phi_{tsm \cdot t + a + a \cdot bill}$	39	16.06	0.00*	0.33
(2) $\Phi_{tsm \cdot t + a + juv \cdot bill}$	38	18.20	0.10	0.31
(3) $\Phi_{tsm \cdot t + a + juv \cdot bill + juv \cdot bill\_sq}$	39	17.91	1.84	0.13
(4) $\Phi_{tsm \cdot t + a + bill}$	38	20.91	2.81	0.08
(5) $\Phi_{tsm \cdot t + a + a \cdot bill + a \cdot bill\_sq}$	41	15.40	3.41	0.06
(6) $\Phi_{tsm \cdot t + a + bill + bill\_sq}$	39	19.98	3.92	0.05
(7) $\Phi_{tsm \cdot t + a + ad \cdot bill}$	38	23.92	5.82	0.02
(8) $\Phi_{tsm \cdot t + a}$	37	27.18	7.04	0.01
(9) $\Phi_{tsm \cdot t + a + ad \cdot bill + ad \cdot bill\_sq}$	39	23.41	7.34	0.01
(10) $\Phi_{tsm \cdot t + a + juv \cdot bill \cdot t}$	49	6.32	10.65	0.00
(11) $\Phi_{tsm \cdot t + a + juv \cdot bill\_class}$	49	10.15	14.49	0.00
(12) $\Phi_{tsm \cdot t + a + ad \cdot bill\_class}$	50	15.78	22.16	0.00
(13) $\Phi_{tsm + a + ad \cdot t + juv \cdot tlin}$	28	66.24	27.84	0.00
(14) $\Phi_{tsm + a + ad \cdot t + juv \cdot snow}$	28	67.25	28.85	0.00
(15) $\Phi_{tsm + a + ad \cdot t + juv \cdot tlin + juv \cdot snow\_detrended}$	29	65.66	29.29	0.00
(16) $\Phi_{tsm \cdot t + a + a \cdot bill\_class}$	62	0.00**	30.99	0.00
(17) $\Phi_{tsm + a + a \cdot t}$	38	49.50	31.40	0.00
(18) $\Phi_{tsm + a + ad \cdot t}$	27	75.77	35.35	0.00
(19) $\Phi_{tsm + a + juv \cdot bill\_class}$	28	93.68	55.28	0.00
(20) $\Phi_{tsm + a + ad \cdot bill\_class}$	29	100.39	64.02	0.00
(21) $\Phi_{tsm + a + a \cdot bill}$	41	82.72	70.73	0.00

*AIC_c = 11407.22
**Deviance = 2403.44

bill = standardized bill length (continuous); bill_sq = bill + $bill^2$; bill_class = bill length rounded off to 1-mm classes (categorical); juv=juvenile (first-year); ad=adult (second-year or older); tlin=year (continuous); snow=date of snowmelt in the previous year; snow_detrended = residual date of snowmelt in the previous year after correcting for the linear trend over time. For explanation of other abbreviations, see Table S6. To calculate the R^2_{dev} as an estimate of the proportion of variation in juvenile survival explained by date of snowmelt, we used the deviances of models 14, 17 and 18 for Dev_{snow}, Dev_t and Dev_{cst}.

Table S8. Resighting and apparent survival probabilities (95% CI in brackets) estimated by the best-supported model from step 1 (model 1, Table S6). This model distinguished between survival of juveniles, of adults in their year after marking (Adult 1) and of adults later on (Adult 2+).

	Resighting probability (p) from July in year *i* to June in year *i*+1		**Apparent survival probability (Φ) from December in year *i*-1 to November in year *i***		
Year *i*	**Abelgh Eiznaya**	**Baie d'Aouatif**	**Juveniles**	**Adult 1**	**Adult 2+**
2003	0.20 (0.14 - 0.28)	0.14 (0.10 - 0.21)	0.53 (0.43 - 0.62)	0.59 (0.50 - 0.67)	No estimate
2004	0.33 (0.27 - 0.40)	0.25 (0.20 - 0.32)	0.72 (0.59 - 0.82)	0.77 (0.64 - 0.86)	1.00 (1.00 - 1.00)
2005	0.38 (0.32 - 0.43)	0.29 (0.23 - 0.35)	0.60 (0.49 - 0.69)	0.65 (0.56 - 0.74)	0.81 (0.67 - 0.90)
2006	0.54 (0.48 - 0.60)	0.44 (0.37 - 0.51)	0.66 (0.53 - 0.77)	0.71 (0.60 - 0.80)	0.92 (0.74 - 0.98)
2007	0.49 (0.43 - 0.54)	0.39 (0.33 - 0.45)	0.56 (0.45 - 0.67)	0.62 (0.52 - 0.71)	0.76 (0.66 - 0.84)
2008	0.45 (0.40 - 0.50)	0.35 (0.30 - 0.41)	0.58 (0.50 - 0.66)	0.64 (0.55 - 0.72)	0.82 (0.70 - 0.89)
2009	0.49 (0.43 - 0.54)	0.39 (0.34 - 0.44)	0.71 (0.59 - 0.81)	0.76 (0.66 - 0.84)	0.76 (0.67 - 0.84)
2010	0.40 (0.35 - 0.45)	0.31 (0.26 - 0.36)	0.57 (0.45 - 0.67)	0.62 (0.53 - 0.71)	0.83 (0.72 - 0.90)
2011	0.45 (0.40 - 0.51)	0.36 (0.30 - 0.41)	0.25 (0.16 - 0.35)	0.29 (0.20 - 0.40)	0.83 (0.71 - 0.91)
2012	0.32 (0.27 - 0.37)	0.24 (0.19 - 0.29)	0.47 (0.37 - 0.59)	0.53 (0.42 - 0.64)	0.79 (0.67 - 0.88)
2013	0.66 (0.60 - 0.72)	0.57 (0.50 - 0.63)	0.51 (0.39 - 0.63)	0.57 (0.46 - 0.67)	0.78 (0.67 - 0.86)

References and Notes

1. C. Parmesan, G. Yohe, A globally coherent fingerprint of climate change impacts across natural systems. *Nature* **421**, 37–42 (2003). Medline doi:10.1038/nature01286

2. C. Teplitsky, V. Millien, Climate warming and Bergmann's rule through time: Is there any evidence? *Evol. Appl.* **7**, 156–168 (2014). Medline doi:10.1111/eva.12129

3. A. R. Baudron, C. L. Needle, A. D. Rijnsdorp, C. T. Marshall, Warming temperatures and smaller body sizes: Synchronous changes in growth of North Sea fishes. *Glob. Change Biol.* **20**, 1023–1031 (2014). doi:10.1111/gcb.12514

4. J. A. Sheridan, D. Bickford, Shrinking body size as an ecological response to climate change. *Nat. Clim. Change* **1**, 401–406 (2011). doi:10.1038/nclimate1259

5. J. L. Gardner, A. Peters, M. R. Kearney, L. Joseph, R. Heinsohn, Declining body size: A third universal response to warming? *Trends Ecol. Evol.* **26**, 285–291 (2011). Medline doi:10.1016/j.tree.2011.03.005

6. K. D. Rode, S. C. Amstrup, E. V. Regehr, Reduced body size and cub recruitment in polar bears associated with sea ice decline. *Ecol. Appl.* **20**, 768–782 (2010). Medline doi:10.1890/08-1036.1

7. C. Teplitsky, J. A. Mills, J. S. Alho, J. W. Yarrall, J. Merilä, Bergmann's rule and climate change revisited: Disentangling environmental and genetic responses in a wild bird population. *Proc. Natl. Acad. Sci. U.S.A.* **105**, 13492–13496 (2008). Medline doi:10.1073/pnas.0800999105

8. N. B. Metcalfe, P. Monaghan, Compensation for a bad start: Grow now, pay later? *Trends Ecol. Evol.* **16**, 254–260 (2001). Medline doi:10.1016/S0169-5347(01)02124-3

9. M. P. Tingley, P. Huybers, Recent temperature extremes at high northern latitudes unprecedented in the past 600 years. *Nature* **496**, 201–205 (2013). Medline doi:10.1038/nature11969

10. J. A. Screen, I. Simmonds, The central role of diminishing sea ice in recent Arctic temperature amplification. *Nature* **464**, 1334–1337 (2010). Medline doi:10.1038/nature09051

11. T. Piersma, Do global patterns of habitat use and migration strategies co-evolve with relative investments in immunocompetence due to spatial variation in parasite pressure? *Oikos* **80**, 623–631 (1997). doi:10.2307/3546640

12. Materials and methods are available as supplementary materials on *Science* Online.

13. T. Piersma, R. van Aelst, K. Kurk, H. Berkhoudt, L. R. M. Maas, A new pressure sensory mechanism for prey detection in birds: The use of principles of seabed dynamics? *Proc. Biol. Sci.* **265**, 1377–1383 (1998). doi:10.1098/rspb.1998.0445

14. T. Oudman, J. Onrust, J. de Fouw, B. Spaans, T. Piersma, J. A. van Gils, Digestive capacity and toxicity cause mixed diets in red knots that maximize energy intake rate. *Am. Nat.* **183**, 650–659 (2014). Medline doi:10.1086/675759

15. J. A. van Gils, M. van der Geest, J. Leyrer, T. Oudman, T. Lok, J. Onrust, J. de Fouw, T. van der Heide, P. J. van den Hout, B. Spaans, A. Dekinga, M. Brugge, T. Piersma, Toxin

constraint explains diet choice, survival and population dynamics in a molluscivore shorebird. *Proc. Biol. Sci.* **280**, 20130861 (2013). Medline doi:10.1098/rspb.2013.0861

16. R. W. Stein, A. R. Place, T. Lacourse, C. G. Guglielmo, T. D. Williams, Digestive organ sizes and enzyme activities of refueling western sandpipers (*Calidris mauri*): Contrasting effects of season and age. *Physiol. Biochem. Zool.* **78**, 434–446 (2005). Medline doi:10.1086/430038

17. J. L. Pérez-Lloréns, M. Muchtar, F. X. Niell, P. H. Nienhuis, Particulate organic carbon, nitrogen and phosphorus content in roots, rhizomes and differently aged leaves of *Zostera noltii* Hornem. in Oosterschelde Estuary (southwestern Netherlands). *Bot. Mar.* **34**, 319–322 (1991). doi:10.1515/botm.1991.34.4.319

18. J. D. Lebreton, K. P. Burnham, J. Clobert, D. R. Anderson, Modeling survival and testing biological hypotheses using marked animals: A unified approach with case studies. *Ecol. Monogr.* **62**, 67–118 (1992). doi:10.2307/2937171

19. P. E. Jönsson, T. Alerstam, The adaptive significance of parental role division and sexual size dimorphism in breeding shorebirds. *Biol. J. Linn. Soc. Lond.* **41**, 301–314 (1990). doi:10.1111/j.1095-8312.1990.tb00838.x

20. A. J. van Dijk, F. E. de Roder, E. C. L. Marteijn, H. Spiekman, Summering waders on the Banc d'Arguin, Mauritania: A census in June 1988. *Ardea* **78**, 145–156 (1990).

21. H. Schekkerman, I. Tulp, T. Piersma, G. H. Visser, Mechanisms promoting higher growth rate in arctic than in temperate shorebirds. *Oecologia* **134**, 332–342 (2003). Medline doi:10.1007/s00442-002-1124-0

22. H. V. Danks, Life cycles in polar arthropods - flexible or programmed? *Eur. J. Entomol.* **96**, 83–102 (1999).

23. T. T. Høye, E. Post, H. Meltofte, N. M. Schmidt, M. C. Forchhammer, Rapid advancement of spring in the High Arctic. *Curr. Biol.* **17**, R449–R451 (2007). Medline doi:10.1016/j.cub.2007.04.047

24. J. R. Liebezeit, K. E. B. Gurney, M. Budde, S. Zack, D. Ward, Phenological advancement in arctic bird species: Relative importance of snow melt and ecological factors. *Polar Biol.* **37**, 1309–1320 (2014). doi:10.1007/s00300-014-1522-x

25. J. Leyrer, P. Bocher, F. Robin, P. Delaporte, C. Goulvent, E. Joyeaux, F. Meunier, T. Piersma, Northward migration of Afro-Siberian knots *Calidris canutus canutus*: High variability in red knot numbers visiting staging sites on the French Atlantic coast, 1979–2009. *Wader Study Group Bull.* **116**, 145–151 (2009).

26. J. J. Bowden, A. Eskildsen, R. R. Hansen, K. Olsen, C. M. Kurle, T. T. Høye, High-Arctic butterflies become smaller with rising temperatures. *Biol. Lett.* **11**, 20150574 (2015). Medline doi:10.1098/rsbl.2015.0574

27. J. S. Bale, S. A. L. Hayward, Insect overwintering in a changing climate. *J. Exp. Biol.* **213**, 980–994 (2010). Medline doi:10.1242/jeb.037911

28. M. P. Grilli, D. E. Gorla, The spatio-temporal pattern of *Delphacodes kuscheli* (Homoptera: Delphacidae) abundance in central Argentina. *Bull. Entomol. Res.* **87**, 45–53 (1997). doi:10.1017/S0007485300036348

29. M. van Roomen, S. Nagy, R. Foppen, T. Dodman, G. Citegetse, A. Ndiaye, *Status of Coastal Waterbird Populations in the East Atlantic Flyway* (Programme Rich Wadden Sea, Sovon, Wetlands International, Birdlife International, Common Wadden Sea Secretariat, 2015).

30. E. G. Lappo, P. S. Tomkovich, E. Syroechkovskiy, *Atlas of Breeding Waders in the Russian Arctic* (Institute of Geography, Russian Academy of Sciences, 2012).

31. Y. Aharon-Rotman, M. Soloviev, C. Minton, P. Tomkovich, C. Hassell, M. Klaassen, Loss of periodicity in breeding success of waders links to changes in lemming cycles in Arctic ecosystems. *Oikos* **124**, 861–870 (2015). doi:10.1111/oik.01730

32. National Oceanic and Atmospheric Administration (NOAA) National Centers for Environmental Information, www.ncdc.noaa.gov/.

33. Manifold System Release 8 (Manifold, 2007); www.manifold.net/.

34. R Core Team, *R: A Language and Environment for Statistical Computing* (R Foundation for Statistical Computing, 2013).

35. R. D. Brown, D. A. Robinson, Northern Hemisphere spring snow cover variability and change over 1922–2010 including an assessment of uncertainty. *Cryosphere* **5**, 219–229 (2011). doi:10.5194/tc-5-219-2011

36. P. Jönsson, L. Eklundh, Seasonality extraction by function fitting to time-series of satellite sensor data. *IEEE Trans. Geosci. Rem. Sens.* **40**, 1824–1832 (2002). doi:10.1109/TGRS.2002.802519

37. NOAA Center for Satellite Applications and Research, "STAR - Global Vegetation Health Products" (NOAA, 2016); http://www.star.nesdis.noaa.gov/smcd/emb/vci/VH/vh_ftp.php.

38. W. Meissner, Variation in timing of the Siberian knot *Calidris c. canutus* autumn migration in the Puck Bay region (southern Baltic). *Acta Ornithol.* **40**, 95–101 (2005). doi:10.3161/068.040.0205

39. W. Meissner, Stopover strategy of adult and juvenile red knots *Calidris c. canutus* in the Puck Bay, southern Baltic. *Ardea* **95**, 97–104 (2007). doi:10.5253/078.095.0111

40. S. Nebel, T. Piersma, J. van Gils, A. Dekinga, B. Spaans, Length of stopover, fuel storage and a sex-bias in the occurrence of Red Knots *Calidris c. canutus* and *C. c. islandica* in the Wadden Sea during southward migration. *Ardea* **88**, 165–176 (2000).

41. A. J. Prater, J. H. Merchant, J. Vuorinen, *Guide to the Identification and Ageing of Holarctic Shorebirds* (British Trust for Ornithology, 1977).

42. K. P. Burnham, D. R. Anderson, *Model Selection and Multimodel Inference* (Springer, 2002).

43. A. J. Baker, T. Piersma, A. D. Greenslade, Molecular vs. phenotypic sexing in red knots. *Condor* **101**, 887–893 (1999). doi:10.2307/1370083

44. M. W. Dietz, B. Spaans, A. Dekinga, M. Klaassen, H. Korthals, C. van Leeuwen, T. Piersma, Do red knots (*Calidris canutus islandica*) routinely skip Iceland during southward migration? *Condor* **112**, 48–55 (2010). doi:10.1525/cond.2010.090139

45. T. Catry, P. M. Lourenço, R. J. Lopes, C. Carneiro, J. A. Alves, J. Costa, H. Rguibi-Idrissi, S. Bearhop, T. Piersma, J. P. Granadeiro, Structure and functioning of intertidal food webs along an avian flyway: A comparative approach using stable isotopes. *Funct. Ecol.* **30**, 468–478 (2015).

46. J. A. van Gils, M. V. Ahmedou Salem, Validating the incorporation of ^{13}C and ^{15}N in a shorebird that consumes an isotopically distinct chemosymbiotic bivalve. *PLOS ONE* **10**, e0140221 (2015). Medline doi:10.1371/journal.pone.0140221

47. A. Parnell, A. Jackson, "siar: Stable Isotope Analysis in R," R package version 4.2 (R Foundation for Statistical Computing, 2013).

48. J. Leyrer, T. Lok, M. Brugge, A. Dekinga, B. Spaans, J. A. van Gils, B. K. Sandercock, T. Piersma, Small-scale demographic structure suggests preemptive behavior in a flocking shorebird. *Behav. Ecol.* **23**, 1226–1233 (2012). doi:10.1093/beheco/ars106

49. J. Leyrer, T. Lok, M. Brugge, B. Spaans, B. K. Sandercock, T. Piersma, Mortality within the annual cycle: Seasonal survival patterns in Afro-Siberian Red Knots *Calidris canutus canutus*. *J. Ornithol.* **154**, 933–943 (2013). doi:10.1007/s10336-013-0959-y

50. J. R. Conklin, T. Lok, D. S. Melville, A. C. Riegen, R. Schuckard, T. Piersma, P. F. Battley, Declining adult survival of New Zealand Bar-tailed Godwits during 2005–2012 despite apparent population stability. *Emu* 10.1071/MU15058 (2016).

51. G. C. White, K. P. Burnham, Program MARK: Survival estimation from populations of marked animals. *Bird Study* **46**, S120–S139 (1999). doi:10.1080/00063659909477239

52. V. Grosbois, O. Gimenez, J. M. Gaillard, R. Pradel, C. Barbraud, J. Clobert, A. P. Møller, H. Weimerskirch, Assessing the impact of climate variation on survival in vertebrate populations. *Biol. Rev. Camb. Philos. Soc.* **83**, 357–399 (2008). Medline doi:10.1111/j.1469-185X.2008.00047.x

53. J. L. Laake, *RMark: An R Interface for Analysis of Capture-Recapture Data with MARK* (AFSC Processed Report 2013-01, Alaska Fisheries Science Center, National Marine Fisheries Service, 2013).

54. T. Piersma, P. de Goeij, I. Tulp, An evaluation of intertidal feeding habitats from a shorebird perspective: Towards relevant comparisons between temperate and tropical mudflats. *Neth. J. Sea Res.* **31**, 503–512 (1993). doi:10.1016/0077-7579(93)90062-W